Progress In Electromagnetics Research C, Vol. 60, 67–74, 2015

A Novel Dual-Band Balanced Power Amplifier Using Branch-Line Couplers with Four Arbitrary Terminated Resistances

Hua Wang*, Bihua Tang, Yongle Wu, Cuiping Yu, and Yuanan Liu

Abstract—A novel dual-band balanced power amplifier (DBPA) using a pair of branch-line couplers with four arbitrary terminated resistances is designed in this paper. The DBPA operating at 2.02 GHz and 2.6 GHz consists of two identical single-stage class-AB PAs connected in parallel and two branch-line couplers for power division and combination. Due to the usage of branch-line couplers with four arbitrary terminated resistances, the load/source-pull impedance obtained by ADS (Advanced Design System) can be matched to an arbitrary real impedance which decreases the complexity of dual-band matching network of the DBPA. To demonstrate the proposed design, a prototype based on CREE's GaN HEMT CGH40010F is fabricated and measured. The simulated results exhibit 67.9% and 73.6% power-added efficiency (PAE) values with output power of 44.1 and 43.4 dBm at 2.02 GHz and 2.6 GHz, respectively.

1. INTRODUCTION

Nowadays, with the rapid evolution of wireless communication system, great efforts have been devoted to multi-standard and multi-band radio systems. Therefore, dual-band power amplifier (PA) which is widely adopted is heavily needed in the front end of RF systems. Power amplifiers (PAs) consuming the most DC power of circuit systems play a significant role in RF circuits of wireless communication. The important issues on power amplifiers such as output power, efficiency and linearity have been studied deeply in [1–3].

Balanced power amplifier is a popular topology of the amplifiers, which consists of two identical single-stage power amplifiers, input power splitter and output power combiner [4–6]. The benefits of balanced amplifier configuration were first recognized in [7], and the advantages of the balanced power amplifier can be summarized as follows: (1) Any mismatch reflections from the amplifiers pass back through the couplers and appear in anti-phase and therefore cancel at the RF input (or output) port [7]. Therefore, the return loss is eliminated. (2) Single-stage amplifier can operate at the optimal status of flat gain or noise coefficient. (3) The balanced power amplifier remains to operate properly when either of the two identical power amplifiers damages, but the total gain of the circuit decreases by 6 dB. (4) Due to the out-of-phase property, the returned reflected signals at the input port are cancelled. Thus, the bandwidth of the balanced power amplifier reaches an octave or more, which is mainly limited by the bandwidth of branch-line couplers. (5) Balanced power amplifiers are much more stable than single-stage amplifiers. Despite those merits, they also suffer from requirements of large coupler size, cost of using double devices, consumption of more DC power and integration problems.

This paper presents the design, fabrication and measurement results of the DBPA. The remaining sections of this paper are constructed as follows. Section 2 describes the design of main parts of the DBPA, including branch-line couplers for power division and combination, dual-band matching network. Eventually, the simulated and measured results are presented in Sections 3 and 4.

Received 30 October 2015, Accepted 23 November 2015, Scheduled 1 December 2015

* Corresponding author: Hua Wang (wanghua122333@outlook.com).

The authors are with the School of Electronic Engineering, Beijing Key Laboratory of Work Safety Intelligent Monitoring, Beijing University of Posts and Telecommunications, P. O. Box 282, Beijing 100876, China.

2. THE DESIGN OF DUAL-BAND BALANCED POWER AMPLIFIER

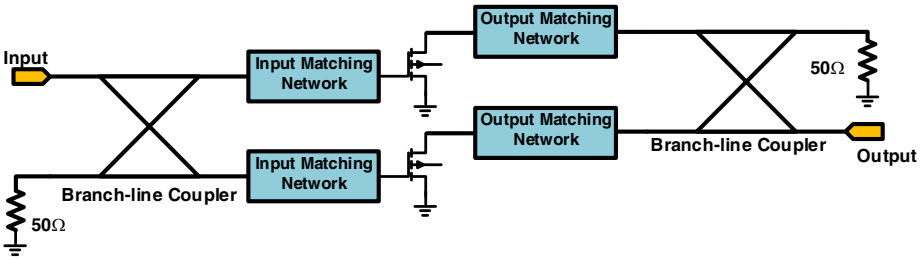

Figure 1. The block diagram of balanced power amplifier.

The structure of the balanced power amplifier is shown schematically in Fig. 1. Two identical power amplifiers are fed from an input power splitter which produces two signals in phase quadrature, and the outputs being recombined using a similar device connected in reverse [7]. In this paper, branch-line couplers are adopted to design splitter and combiner. Since the input and output branch-line couplers can make a phase shift of 90 degrees, respectively, the signal of two power amplifiers in parallel are in-phase stacking. The S-parameters of a balanced power amplifier can be given as follows [8]:

$$S_{11} = |S_{11A} - S_{11B}|/2, \quad (1)$$
$$S_{22} = |S_{22A} - S_{22B}|/2, \quad (2)$$
$$S_{21} = |S_{21A} + S_{21B}|/2, \quad (3)$$
$$S_{12} = |S_{12A} + S_{12B}|/2. \quad (4)$$

2.1. Dual-Band Branch-Line Coupler

The branch-line coupler used as power splitter splits the input signal into two ideally equal and 90 degrees out of phase parts. Then the outputs of the two identical single-stage power amplifiers are combined and brought in phase through power combiner. Due to the dual-band operation of the proposed PA, a dual-band branch-line coupler is necessarily required. In [9], a new design concept of a generalized dual-band branch-line coupler with unequal power division and four arbitrary terminated resistances is reported. Detailed theoretical derivation and design method are exhibited in [9]. The circuit configuration of the dual-band branch-line coupler is shown in Fig. 2. In Fig. 3, the simulated scattering parameters of the coupler are given, indicating a good return loss and high isolation. Meanwhile, port 2 and port 3 output equal power at a broadband of 2.02 GHz and 2.6 GHz. The phase difference of port 2 and port 3 is about 90 ± 2 degrees.

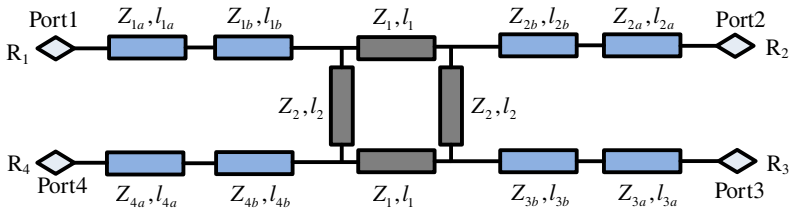

Figure 2. Circuit schematic of dual-band branch-line coupler.

2.2. Dual-Band Matching Network

First of all, a dual-band class AB power amplifier utilizing CREE's GaN CGH40010F is designed. In the procedure of designing power amplifier, the performance of the matching network directly determines the power amplifier's output power, efficiency, bandwidth, etc. Due to the dual-band operation of the

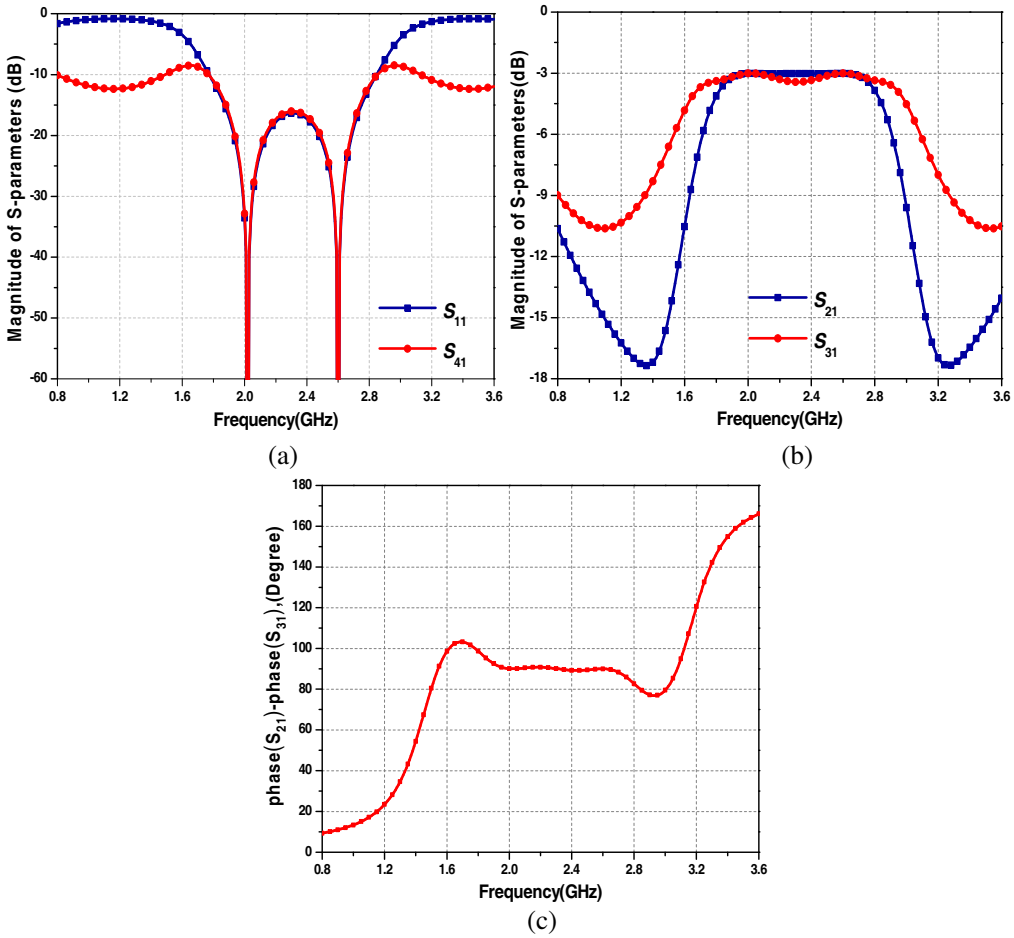

Figure 3. Simulated scattering parameters of the dual-band branch-line coupler: (a) matching and isolation; (b) transmission; (c) phase difference.

balanced power amplifier, its input/output matching network differs from the power amplifiers that operate at single band. In this paper, the design of dual-band impedance matching network is on the basis of a three-section transformer for frequency-dependent complex load impedance matching [10–12]. It is mentioned in Subsection 2.1 that the adopted dual-band branch-line couplers can be terminated with four arbitrary resistances. Therefore, it is simplified to match the load/source pull impedance to arbitrary resistances rather than 50 Ω. Then a relative simple dual-band impedance matching network is easy to obtain. For appropriate complex impedances, the dual-band impedance matching network can be implemented by a two-section transformer.

The transformer comprises two sections (Section 1 and Section 2 with characteristic impedances Z_1, Z_2 and physical lengths l_1, l_2 respectively) as illustrated in Fig. 4. The two irrelevant complex load

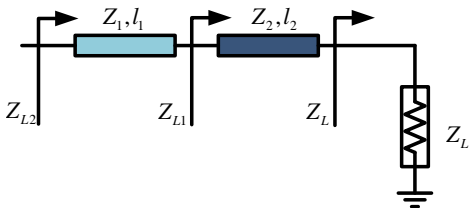

Figure 4. Configuration of two-section transformer.

impedances are defined as R_a+jX_a and R_b+jX_b at f_1 and f_2 (assuming $f_2 = mf_1$, $m \geq 1$), respectively. The subscripts a and b denote two frequencies f_1 and f_2, respectively. The first step is to match the complex load impedances under two frequencies f_1 and f_2 to a pair of conjugated impedances. Based on the transmission line impedance equation

$$Z_{in} = Z_0 \frac{Z_L + jZ_0 \tan(\beta l)}{Z_0 + jZ_L \tan(\beta l)}. \tag{5}$$

The input impedance Z_{L1} at f_1 and f_2 can be defined as ($\beta_f = 2\pi/\lambda_f$, $\beta_{f2} = m\beta_{f1}$)

$$Z_{L1}|f_1 = Z_2 \frac{R_a + jX_a + jZ_2 \tan(\beta_{f1} l_2)}{Z_2 + j(R_a + jX_a)\tan(\beta_{f1} l_2)}. \tag{6}$$

$$Z_{L1}|f_2 = Z_2 \frac{R_b + jX_b + jZ_2 \tan(\beta_{f2} l_2)}{Z_2 + j(R_b + jX_b)\tan(\beta_{f2} l_2)}. \tag{7}$$

According to the relationship $Z_{L1}|f_1 = (Z_{L1}|f_2)^*$, hereby the following Equations (8) and (9) can be derived

$$Z_2 = \sqrt{R_a R_b + X_a X_b + \frac{X_a + X_b}{R_b - R_a}(R_a X_b - R_b X_a)}. \tag{8}$$

$$l_2 = \frac{n\pi + \arctan\left[\dfrac{Z_2(R_a - R_b)}{R_a X_b - R_b X_a}\right]}{(m+1)\beta_{f1}}. \tag{9}$$

Once Section 2 is determined, Z_{L1} can be computed. The remaining work is to match this pair of conjugated impedances to an appropriate resistance. It is assumed that

$$\begin{cases} Z_{L1} = R_{L1} + jX_{L1}, \ @f_1 \\ Z_{L1} = R_{L1} - jX_{L1}, \ @f_2 \end{cases}. \tag{10}$$

It is easy to obtain Equations (11) and (12)

$$Z_{L2}|f_1 = Z_1 \frac{R_{L1} + jX_{L1} + jZ_1 \tan(\beta_{f1} l_1)}{Z_1 + j(R_{L1}+jX_{L1})\tan(\beta_{f1} l_1)}. \tag{11}$$

$$Z_{L2}|f_2 = Z_1 \frac{R_{L1} - jX_{L1} + jZ_1 \tan(\beta_{f2} l_1)}{Z_1 + j(R_{L1} - jX_{L1})\tan(\beta_{f2} l_1)}. \tag{12}$$

Make sure that the imaginary parts of $Z_{L2}|f_1$ and $Z_{L2}|f_2$ are equal to zero. At the same time, the real part of $Z_{L2}|f_1$ and $Z_{L2}|f_2$ are equal. From (10), (11) and (12), we establish

$$\tan(\beta_{f1} l_1) + \tan(\beta_{f2} l_1) = 0. \tag{13}$$

whose roots are infinite for l_1. To implement a matching structure as compact as possible, we choose

$$l_1 = \frac{\pi}{\beta_{f1} + \beta_{f2}}. \tag{14}$$

Meanwhile, the equation for Z_1 can be deduced by eliminating variables

$$Z_1^2 + 2X_{L1}\tan(2\theta_1)Z_1 - (X_{L1}^2 + R_{L1}^2) = 0. \tag{15}$$

To solve Equation (16), we have the expression of Z_1 as Equation (16).

$$Z_1 = \frac{-b \pm \sqrt{b^2 - 4ac}}{2a}. \tag{16}$$

Variable definitions of Equations (15) and (16) are shown in Equation (17)

$$\begin{cases} a = 1 \\ b = \dfrac{X_{L1}(1 - \tan^2(\theta_1))}{\tan(\theta_1)} \\ c = -(R_{L1}^2 + X_{L1}^2) \\ \theta_1 = \dfrac{\pi f_1}{f_1 + f_2} \end{cases}. \tag{17}$$

To validate the effectiveness of the two-section transformer, the output matching network is taken as an example. At two frequencies 2.02 GHz and 2.6 GHz, the load-pull impedances through ADS (Advanced Design System) are $(13.70 - j * 10.26)\,\Omega$ and $(11.06 - j * 6.00)\,\Omega$, respectively. Then the conjugations of the load-pull impedances are matched to the same resistance utilizing two-section transformer as shown in Fig. 5. It is derived that the characteristic impedances and physical lengths of the two sections can be derived as $Z_1 = 41.1\,\Omega$, $Z_2 = 20.2\,\Omega$, $l_1 = 19.3\,\text{mm}$, $l_2 = 12.4\,\text{mm}$, through theoretical analysis above. The resistance Z is $41\,\Omega$. In Fig. 6, the simulated scattering parameters show that the return loss S_{11} is less than $-40\,\text{dB}$ and transmission coefficient close to $0\,\text{dB}$ in a wide range of the two frequency points. It sufficiently proves that the performance of the matching network is excellent.

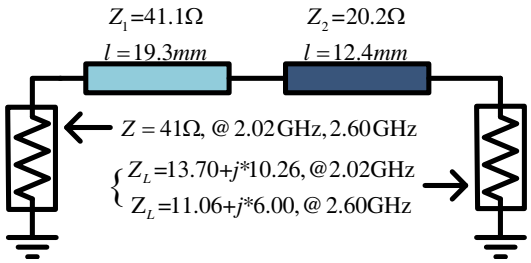

Figure 5. Output matching network.

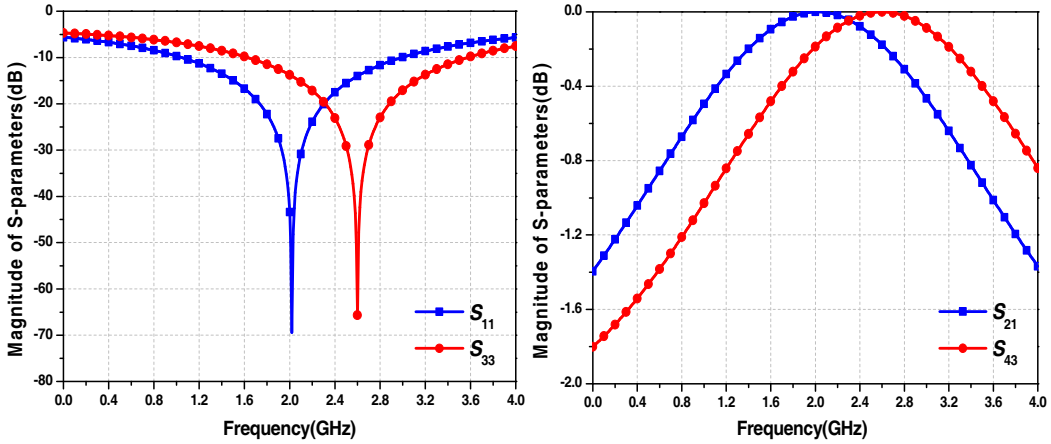

(a) (b)

Figure 6. Simulated scattering parameters of the dual-band matching network: (a) return loss (b) transmission.

In practice, not all of the two arbitrary independent complex impedances can be matched to a same resistance through the two-section transformer. To overcome this shortfall, a general way is to add a shunt open stub or a series microstrip to transform these two impedances to appropriate impedances. Hereto, it is convenient to implement the proposed dual-band class AB PA based on the proposed theoretical analysis of the matching network.

3. FABRICATION AND MEASUREMENT

The designed DBPA is fabricated using a Rogers4350B substrate with a dielectric constant of 3.48 and height of 0.762 mm. The overall circuit size is about $250 \times 130\,\text{mm}^2$. Fig. 7 shows a photograph of the final fabricated DBPA. Due to the difference of transistors characteristics, the gate and drain biases of the two transistors are set at $V_{gs} = -2.4\,\text{V}$, $-2.5\,\text{V}$ and $V_{ds} = 28\,\text{V}$, respectively.

The measured and simulated results of the DBPA are depicted in Figs. 8–11. Fig. 8 shows the comparison of simulated and measured S-parameters of the DBPA which features the small-signal gain of 12.5 and 10.8 dB, input return loss of 32.2 and 21.3 dB at 2.02 and 2.47 GHz, respectively in practical measurement. As depicted, the second frequency of the design shifts in frequency by about 100 MHz, but the measurement results clearly confirm dual-band performance. The discrepancy between the

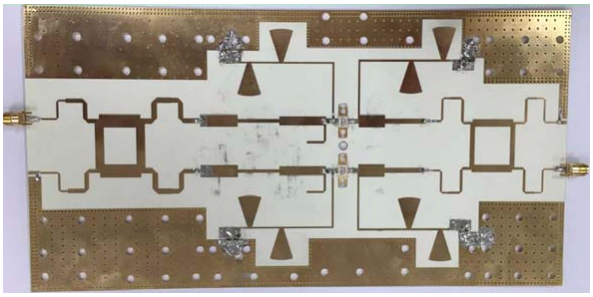

Figure 7. The photograph of the fabricated DBPA.

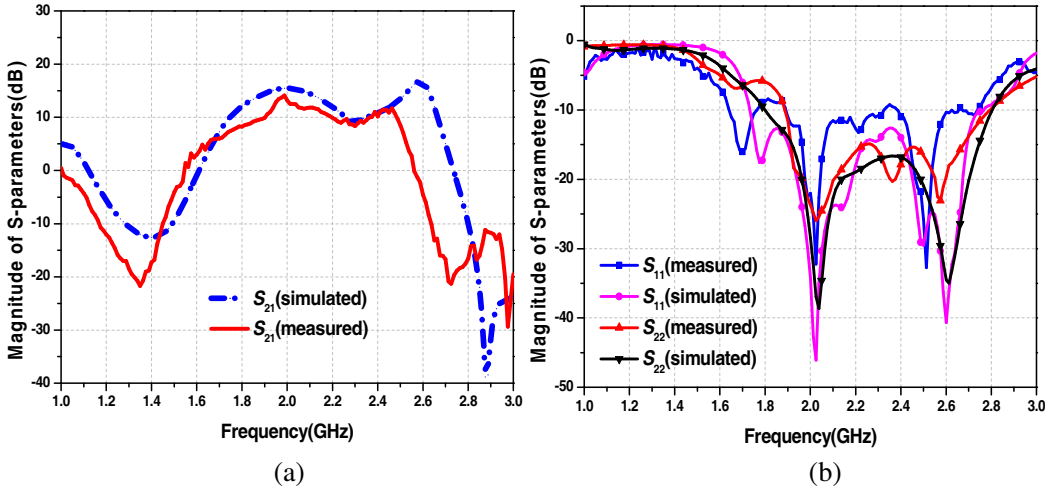

Figure 8. Measured and simulated S-parameters of the DBPA: (a) transmission, (b) return loss.

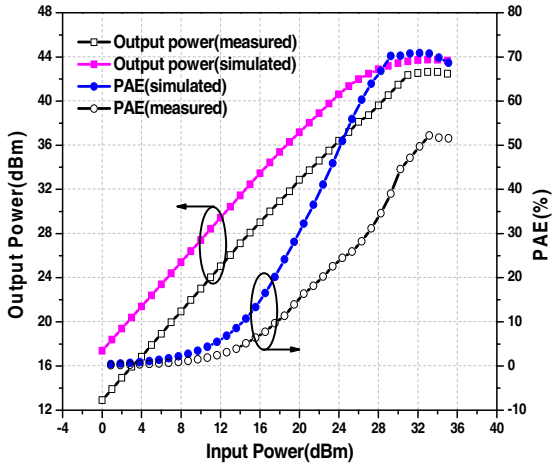

Figure 9. Measured and simulated output power and PAE of the DBPA at 2.02 GHz.

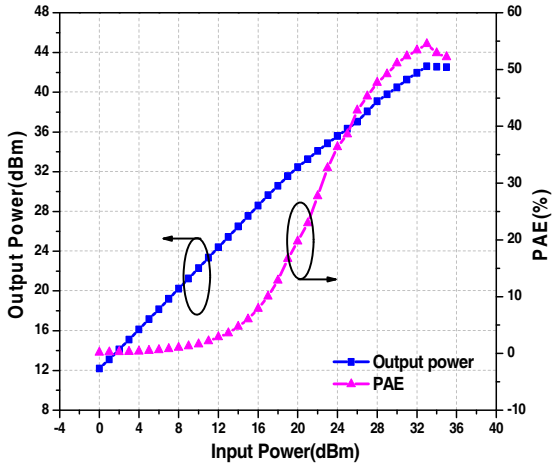

Figure 10. Measured output power and PAE of the DBPA at 2.47 GHz.

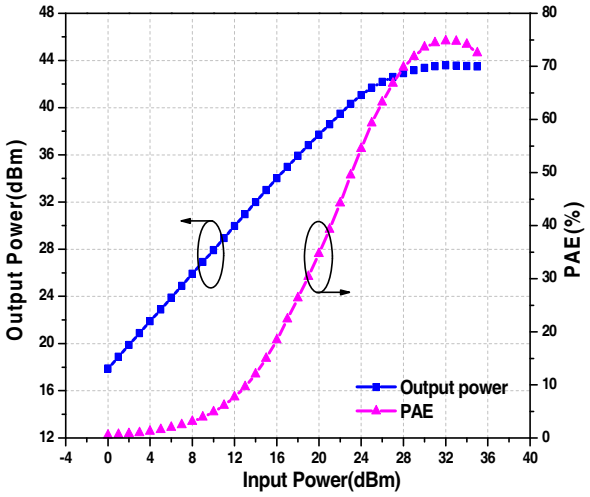

Figure 11. Simulated output power and PAE of the DBPA at 2.6 GHz.

Table 1. Performance comparison.

Work	Frequency (GHz)	Device	PAE (%)	Max P_{out} (dBm)
[1]	2.14	/	29	33
[3]	3.3–3.7	GaN	47(51)	39(42)
[4]	2	LDMOS	38.5	47
[8]	1.85–2.14	LDMOS	35.5(42.5)	47
This work	**2.02/2.47**	**GaN**	**52.2/54.5**	**43.4/42.2**

measurement and simulation is primarily attributed to poor output matching and out of phase of two signals in parallel through the couplers, which bring about high sensitivity of the PA's gain to load impedance variations. Meanwhile, all the microstrip line lengths are engineered for 2.02 GHz. Hence, large-signal performance is more accurate in this band. Finally, the machining accuracy and deviation from ideal conditions also worsen the PA's performance.

Figures 9–11 mainly show large-signal characteristics of the DBPA. At 2.02 GHz, a power gain of 12.9 dB with saturated output power of 43.4 dBm and PAE of 52.2% is achieved. As said above, the second frequency of the measurement deviates from that of simulation about 130 MHz. At 2.47 GHz, the power gain reaches about 12.2 dB with saturated output power of 42.2 dBm and PAE of 54.5%. The simulated output power and PAE of the DBPA at 2.6 GHz is also depicted in Fig. 11. As reported in Table 1, the proposed DBPA exhibits competitive performance compared with other research works especially in the application of dual bands.

4. CONCLUSIONS

A novel dual-band balanced power amplifier with branch-line coupler terminated with four arbitrary resistances has been proposed in this paper. This proposed circuit configuration includes two identical dual-band class AB PAs and two dual-band branch-line couplers. Meanwhile, a microstrip prototype of the DBPA is fabricated and measured for the purpose of complete verification. The fabricated amplifier achieves more than 42 dBm of output power and over 50% of power added efficiency in both bands. To the authors' best knowledge, this is the first reported dual-band balanced power amplifier in open literatures. The measured results do not show great consistence with the theoretical simulation due to various reasons. Nevertheless, it also indicates that the proposed DBPA can be utilized in multi-band wireless communication systems. It is essential to point out that the complete design procedure is based on strict theoretical derivation.

ACKNOWLEDGMENT

This work was supported in part by the National Key Basic Research Program of China (973 Program) (No. 2014CB339900) and National Natural Science Foundation of China (Nos. 61422103, 61327806).

REFERENCES

1. Lim, J., C. Park, J. Koo, H. Cha, Y. Jeong, S. Han, and D. Ahn, "A balanced power amplifier utilizing the reflected input power," *IEEE International Symposium on Radio-Frequency Integration Technology*, Jan. 2009.
2. Gao, L., X. Zhang, S. Chen, and Q. Xue, "Compact power amplifier with band-pass response and high efficiency," *IEEE Microwave and Wireless Components Letters*, Vol. 24, No. 10, 707–709, Oct. 2014.
3. Kizilbey, O. and O. Palamutcuogullari, "Design of 3.3–3.7 GHz GaN HEMT balanced class E power amplifier," *Proceedings of the 7th International Conference Onelectrical and Electronics Engineering*, Dec. 2011.
4. Dettmann, I., L. Wu, and M. Berroth, "Comparison of a single-ended class AB, a balance and a doherty power amplifier," *Proceedings of Asia-Pacific Microwave Conference*, Dec. 2005.
5. Eisele, K., R. Engelbrecht, and K. Kurokawa, "Balanced transistor amplifiers for precise wideband microwave applications," *Proceedings of Solid State Circuits Conference*, Feb. 1965.
6. Hou, Z., and L. Chiu, "A dual-band balanced amplifier using three-layer technology," *Microwaveand Optical Technology Letters*, Vol. 56, No. 7, 1680–1683, Jul. 2014.
7. Cripps, S. C., *RF Power Amplifier Wireless Communication*, 380–387, Artech House, 1999.
8. Wu, L., U. Basaran, I. Dettmann, M. Berroth, T. Bitzer, and A. Pascht, "A broadband high efficiency class-AB LDMOS balanced power amplifier," *Proceeding of European Microwave Conference*, Oct. 2005.
9. Wu, Y., S. Zheng, S. Leung, Y. Liu, and Q. Xue, "An analytical design method for a novel dual-band unequal coupler with four arbitrary terminated resistances," *IEEE Transactionon Industrial Electronics*, Vol. 61, No. 10, 5509–5516, Oct. 2014.
10. Liu, X., Y. Liu, S. Li, F. Wu, and Y. Wu, "A three-section dual-band transformer for frequency-dependent complex load impedance," *IEEE Microwaveand Wireless Components Letters*, Vol. 19, No. 10, 611–613, Oct. 2009.
11. Monzon, C.,"A small dual-frequency transformerin two sections," *IEEE Transaction. Microwave Theory and Techniques*, Vol. 51, No. 4, 1157–1161, Apr. 2003.
12. Wu, Y., Y. Liu, S. Li, C. Yu, and X. Liu, "A generalized dual-frequency transformer for two arbitrary complex frequency-dependent impedances," *IEEE Microwave and Wireless Components Letters*, Vol. 19, No. 12, 792–794, Dec. 2009.